Optical characterization of ground states of polyacene

Shoji Yamamoto
Department of Physics, Hokkaido University, Sapporo 060-0810, Japan
(Received 15 September 2008; published 18 December 2008)

We investigate the ground-state properties of polyacene in terms of an extended Peierls-Hubbard Hamiltonian with particular emphasis on its structural instability of two types: double bonds in a *cis* pattern and those in a *trans* pattern. Calculating the polarized optical conductivity spectra within and beyond the Hartree-Fock scheme, we reveal a striking contrast between the *cis* and *trans* configurations. The two Peierls-distorted states are almost degenerate in their energetics but quite distinct in their optics.

DOI: 10.1103/PhysRevB.78.235205 PACS number(s): 78.30.Jw, 78.20.Bh, 63.20.kd, 78.20.Ci

I. INTRODUCTION

There is a lot of enthusiasm for semiconducting organic materials, which are available at low cost, easy to process, lightweight, and flexible. Especially for the last few decades, particular attention has been paid to polyacene oligomers, consisting of an aromatic (AM) linear array, due to their multifunctional electronic properties. Tetracene and pentacene, for instance, serve as light-emitting devices[1,2] and field-effect transistors.[3–5] The recent discovery of graphene[6] and the success of patterning it into a narrow ribbon[7–9] have stimulated a renewed interest[10] in polyacene as a basic building unit of them.

Prior to the advent of the modern microelectronics, few scientists were already interested in the energy structure of polyacene from a theoretical point of view. Early investigations, initiated by Salem and Longuet-Higgins,[11] focused on the ground state of polyacene—whether and how the Peierls distortion occurs. The discussion was more and more activated with the fabrication of highly conductive *trans*-polyacetylene.[12] There may be a structural instability in polyacene,[11] as well as in polyacetylene,[13] on a qualitatively distinct mechanism,[14] however. Although much effort has so far been devoted to predicting which structure is energetically preferable in polyacene, *cis*-distorted, *trans*-distorted, or uniform (cf. Fig. 1), this long-standing problem is not yet fully settled. Every structure was actually nominated for the most stable in the literature.[15] The controversy suggests that all these structures should closely compete with each other.

First of all the *cis*- and *trans*-distorted isomers of infinite polyacene have exactly the same energy within an electron-phonon model without any Coulomb interaction[16] such as the Su-Schrieffer-Heeger (SSH) Hamiltonian for polyacetylene.[17] They remain degenerate with each other unless we take account of Coulomb interactions beyond the Hartree-Fock (HF) scheme. Second the Peierls instability in polyacene is conditional for both *cis* and *trans* forms,[11,18] where the electron-phonon coupling strength seriously affects the scenario. Third, electron correlations make the situation more difficult.[19] On one hand, they enhance the Peierls instability, while they push the Mott-Hubbard antiferromagnetic insulator, on the other hand, against the uniform aromatic configuration.

In such circumstances, Ramasesha and co-workers[18,19] applied modern numerical tools to polyacene modeled on correlated Hamiltonians of the Hubbard and Pariser-Parr-Pople (PPP) types, which include the on-site repulsion alone and the power-law-decaying long-ranged interaction whole, respectively, but both take no account of spontaneous phonons. They claim that the *cis* distortion is lower in energy than the *trans* one, both of which may, however, be replaced by a spin-density wave on the uniform lattice with increasing Coulomb interactions. While other authors[20–22] predicted a fully delocalized nonalternating nature of polyacene employing standard and developed density-functional methods, the energy difference among such competing states must be

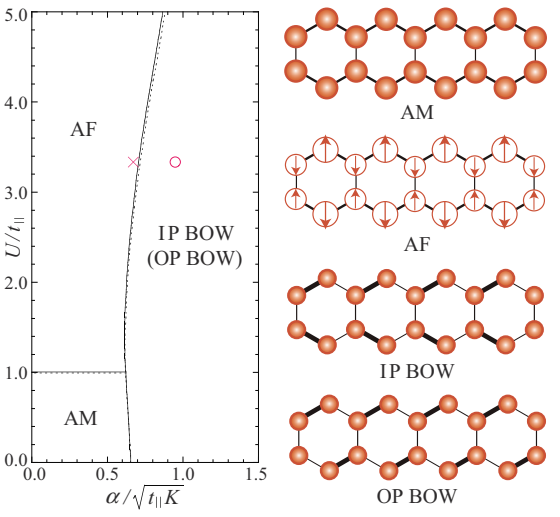

FIG. 1. (Color online) HF (dotted lines) and single-double-excitation configuration-interaction (SDCI) (solid lines) calculations of a ground-state phase diagram on the α-U plain at $N=16$ under the screened-Coulomb parametrization. × and ○ indicate the two sets of model parameters considered here. We find a metallic state of AM configuration, an antiferromagnetic (AF) Mott insulator, and *cis*- and *trans*-distorted Peierls insulators, which read as in-phase (IP) and out-of-phase (OP) bond-order-wave (BOW) states, respectively. All the phases obtained are schematically illustrated, where various segments qualitatively represent the variation in local bond orders, while arrows in circles depict the alternation of local spin densities. IP and OP BOWs are degenerate with each other within the HF scheme, whereas IP BOW is slightly favored over OP BOW in the SDCI scheme.

rather small[15] in any case. Then distorted and undistorted regions may coexist in actual polyacene compounds due to inevitable local defects and/or possible thermal excitations. We are now led to take an interest in characterizing these likely states rather than ranking them. Even if there is a slight energy difference between the *cis*- and *trans*-distorted structures, how can we tell the lower from the higher in practice? We suggest the polarized optical spectroscopy for polyacene in answer to this question.

It deserves special mention in the context of our interest that Sony and Shukla[23] recently calculated the optical-absorption spectra of oligoacenes on a large scale within correlated Hamiltonians of the PPP type. Starting from the restricted HF state, which is an undistorted paramagnetic metal, they investigated in detail configuration interactions (CIs) between its particle-hole excitations of various levels—single, double, and more. In order to describe the effects of electron correlations on the optical properties of aromatic molecules as precisely as possible, their argument was restricted to small oligomers up to seven benzene rings and any possibility of lattice distortion was ruled out. Other groups of theoreticians[16,24–29] investigated an infinite acene chain within uncorrelated models of the SSH type in an attempt to find nonlinear excitations such as solitons and polarons, where any scenario is constructed on a Peierls-distorted structure without any concern for its configuration—*cis* or *trans*—because of the degenerate energetics. Thus and thus, there is, to our knowledge, no guiding calculation of the optical properties of polyacene under both electron-electron and electron-lattice interactions adequately existent.

II. MODELING AND FORMULATION

We aim at revealing the generic behavior of polyacene rather than listing individual features of small oligoacenes. In order to simulate an infinite chain efficiently, we adopt the periodic boundary condition and restrict Coulomb interactions to a certain range. Srinivasan and Ramasesha[19] investigated the ground-state properties of polyacene applying a projector Monte Carlo method to the Hubbard Hamiltonian with periodic boundaries, while Raghu *et al.*[18] carried out similar calculations applying a density-matrix renormalization-group method to the PPP Hamiltonian with open boundaries. They declared that the long-range nature of electron-electron interactions does not qualitatively affect their essential findings such as the conditional Peierls instability and the *cis* distortion being favored over the *trans* one. Sony and Shukla[23] further demonstrated that even the Hückel modeling succeeds in reproducing some aspects of the linear optical spectra of fully correlated oligoacenes modeled on the PPP Hamiltonian. The low-lying optical absorptions are well describable with both Hückel and PPP models, though the Hückel scheme considerably underestimates the optical gap in general.

Thus convinced, we depict polyacene in terms of an extended Peierls-Hubbard Hamiltonian,

$$\begin{aligned}\mathcal{H} = &-\sum_{l=1}^{2}\sum_{n=1}^{N}\sum_{s=\pm}\left[(t_{\parallel}-\alpha r_{l:2n-1})c_{l:2n-1,s}^{\dagger}c_{l:2n,s}+(t_{\parallel}-\alpha r_{l:2n})c_{l:2n,s}^{\dagger}c_{l:2n+1,s}+\mathrm{H.c.}\right]-t_{\perp}\sum_{n=1}^{N}\sum_{s=\pm}(c_{1:2n-1,s}^{\dagger}c_{2:2n-1,s}+\mathrm{H.c.})\\ &+\frac{K}{2}\sum_{l=1}^{2}\sum_{n=1}^{N}(r_{l:2n-1}^{2}+r_{l:2n}^{2})+U\sum_{l=1}^{2}\sum_{n=1}^{N}\left[\left(n_{l:2n-1,+}-\frac{1}{2}\right)\left(n_{l:2n-1,-}-\frac{1}{2}\right)+\left(n_{l:2n,+}-\frac{1}{2}\right)\left(n_{l:2n,-}-\frac{1}{2}\right)\right]\\ &+V_{\parallel}\sum_{l=1}^{2}\sum_{n=1}^{N}\sum_{s,s'=\pm}\left(n_{l:2n,s}-\frac{1}{2}\right)(n_{l:2n-1,s'}+n_{l:2n+1,s'}-1)+V_{\perp}\sum_{n=1}^{N}\sum_{s,s'=\pm}\left(n_{1:2n-1,s}-\frac{1}{2}\right)\left(n_{2:2n-1,s'}-\frac{1}{2}\right),\end{aligned}\tag{2.1}$$

where $c_{l:j,s}^{\dagger}$ and $c_{l:j,s}$ ($c_{l:j,s}^{\dagger}c_{l:j,s}\equiv n_{l:j,s}$) create and annihilate, respectively, a π electron of spin $s=\uparrow,\downarrow\equiv\pm$ at site j on chain l, while $r_{l:j}$ denotes the bond distortion caused by the jth and $(j+1)$th carbon atoms in the lth chain on the description of polyacene as a couple of *trans* isomers of polyacetylene with interchain bonding at every other site. The Coulomb interactions, ranging over neighboring sites, are modeled in $V_{\parallel(\perp)}=U/\kappa\sqrt{1+0.6117a_{\parallel(\perp)}^{2}}$ (Ref. 30) where κ is a dielectric parameter, while $a_{\parallel}$ and $a_{\perp}$ are the average lengths in angstroms of neighboring C–C leg and rung bonds, respectively. Keeping the screened-Coulomb parameters in mind, which were initiated by Chandross and Mazumdar[31] and successfully applied to oligoacenes by Sony and Shukla,[23] we adopt $U=8.0$ eV with $\kappa=2.0$. Though the Coulomb interactions in our use are not infinitely ranged but cut off, such a parametrization must be suggestive and convincing under long-range correlations of merely moderate effect.[18] The intrachain and interchain electron hoppings are described by $t_{\parallel}$ and $t_{\perp}$, respectively. We take 2.4 eV for $t_{\parallel}$ (Ref. 23) and set $t_{\perp}$ equal to $0.864t_{\parallel}$,[26–29] considering that $a_{\parallel}\simeq 1.4$ Å $<a_{\perp}\simeq 1.5$ Å.[21,32] α characterizes the electron-lattice coupling with K being the σ-bond elastic constant. We use, unless otherwise noted, $\alpha=4.1$ eV/Å and $K=15.5$ eV/Å^2.[16,24–29]

In order to calculate the polarized optical conductivity spectra of polyacene, we define current operators along the long and short axes as

$$\mathcal{J}_{\parallel} = \frac{\sqrt{3}iea_{\parallel}}{2\hbar}\sum_{l,n,s}[(t_{\parallel} - \alpha r_{l:2n-1})c^{\dagger}_{l:2n-1,s}c_{l:2n,s} + (t_{\parallel} - \alpha r_{l:2n})c^{\dagger}_{l:2n,s}c_{l:2n+1,s} - \text{H.c.}], \quad (2.2)$$

$$\mathcal{J}_{\perp} = \frac{iea_{\parallel}}{2\hbar}\sum_{l,n,s}(-1)^{l}[(t_{\parallel} - \alpha r_{l:2n-1})c^{\dagger}_{l:2n-1,s}c_{l:2n,s} - (t_{\parallel} - \alpha r_{l:2n})c^{\dagger}_{l:2n,s}c_{l:2n+1,s} - \text{H.c.}] + \frac{iea_{\perp}}{\hbar}\sum_{n,s} t_{\perp}(c^{\dagger}_{1:2n-1,s}c_{2:2n-1,s} - \text{H.c.}). \quad (2.3)$$

Since the charge-transfer excitation energy is of eV order, the system effectively lies in the ground state at room temperature. Then the real part of the optical conductivity reads

$$\sigma_{\parallel,\perp}(\omega) = \frac{\pi}{\omega}\sum_{i}|\langle E_i|\mathcal{J}_{\parallel,\perp}|E_0\rangle|^2\delta(E_i - E_0 - \hbar\omega), \quad (2.4)$$

where $|E_i\rangle$ denotes a wave vector of the ith-lying state of energy E_i. The state vectors are calculated within and beyond the HF scheme being generally defined as

$$|E_i\rangle = |E_0\rangle_{\text{HF}} + \sum_{m(k,\mu,s)=1}^{4N}\sum_{m(k,\nu,s)=4N+1}^{8N} f(k,\mu,\nu,s;i)a^{\dagger}_{m(k,\nu,s)}a_{m(k,\mu,s)}|E_0\rangle_{\text{HF}} + \sum_{m(k_1,\mu_1,s_1)>m(k_2,\mu_2,s_2)=1}^{4N}\sum_{m(k_1,\nu_1,s_1)>m(k_2,\nu_2,s_2)=4N+1}^{8N} f(k_1,k_2,\mu_1,\mu_2,\nu_1,\nu_2,s_1,s_2;i) \times a^{\dagger}_{m(k_1,\nu_1,s_1)}a^{\dagger}_{m(k_2,\nu_2,s_2)}a_{m(k_1,\mu_1,s_1)}a_{m(k_2,\mu_2,s_2)}|E_0\rangle_{\text{HF}}, \quad (2.5)$$

where $|E_0\rangle_{\text{HF}} \equiv \Pi_{m=1}^{4N}a^{\dagger}_{m}|0\rangle$ is the ground-state HF wave function with $|0\rangle$ being the true electron vacuum and $a^{\dagger}_{m}$ creating an electron in the mth HF orbital of energy ε_m. The orbital label m is a function of momentum k, band label λ, and spin s, which are all good quantum numbers here. Any transition of finite momentum transfer is optically forbidden, which serves to reduce the number of configurations to take into calculation. Every excited state of the HF type is a single Slater determinant,[33] where $f(k,\mu,\nu,s;i) = \delta_{k\mu\nu s,i}$, $f(k_1,k_2,\mu_1,\mu_2,\nu_1,\nu_2,s_1,s_2;i) = 0$, and thus $E_i = {}_{\text{HF}}\langle E_0|\mathcal{H}|E_0\rangle_{\text{HF}} - \varepsilon_{m(k,\mu,s)} + \varepsilon_{m(k,\nu,s)}$. Those of the CI type consist of resonating Slater determinants,[34] where the coefficients are determined so as to diagonalize the original Hamiltonian (2.1). Within the single-excitation CI (SCI) scheme, $f(k_1,k_2,\mu_1,\mu_2,\nu_1,\nu_2,s_1,s_2;i)$ remains vanishing, and therefore, no excited-state Slater determinant mixes with the ground-state one, $|E_0\rangle = |E_0\rangle_{\text{HF}}$. When we proceed to the single-double-excitation configuration interaction (SDCI) scheme, there occurs a significant correction to the ground-state energy as well as to every excited-state one. The CI method enables us to systematically investigate many-body effects beyond the HF approximation in fairly large systems that we can hardly diagonalize directly. It was indeed successfully applied to oligoacenes[23] and related phenyl-based conjugated polymers[35–40] with its expansion truncated at varying level.

III. GROUND-STATE PHASE COMPETITION

Even though we take particular interest in the optical features of polyacene as a Peierls insulator, it is still important for us to have a bird's-eye view of its competing ground states. We calculate their energies at the HF and SDCI levels and visualize the ground-state phase competition in Fig. 1. Besides Peierls-distorted structures, which are referred to here as IP and OP BOW states, we find two undistorted structures, a metallic state of AM configuration and a Mott-insulating state of AF configuration. AM is fully symmetric and has no band gap at the HF level. It has a gap in the SDCI scheme, however. AF is more stabilized and wider gapped with increasing on-site Coulomb repulsion. There is another undistorted structure possible, which is characterized as a charge-density wave (CDW),[41] but it is not stabilized into the ground state under the screened-Coulomb parametrization. CDW is realized when we adopt a standard-Coulomb parametrization,[23] which is, however, inferior in reproducing experimental findings.[35–40]

The HF energies of IP and OP BOWs are the same. IP BOW gains more correlation energy than OP BOW in the SDCI scheme. However, their energy difference is small and decreases with increasing conjugation length. IP and OP BOWs are highly degenerate with each other in sufficiently long acene chains. They are stabilized conditionally, that is, depending on the electron-lattice coupling strength, against AM and AF under weak and strong electron-electron correlations, respectively. Moderate Coulomb interactions enhance the Peierls instability. The realistic parameters in our use, which are indicated with $\times$ in Fig. 1, sit in close vicinity to a phase boundary. The ground state is a Mott insulator, but it closely competes with Peierls insulators. Many-body electron correlations seem to contribute toward a closer competition between them. They are very much likely to coexist in polyacene.[42] Then, how can we distinguish between the two distorted structures?

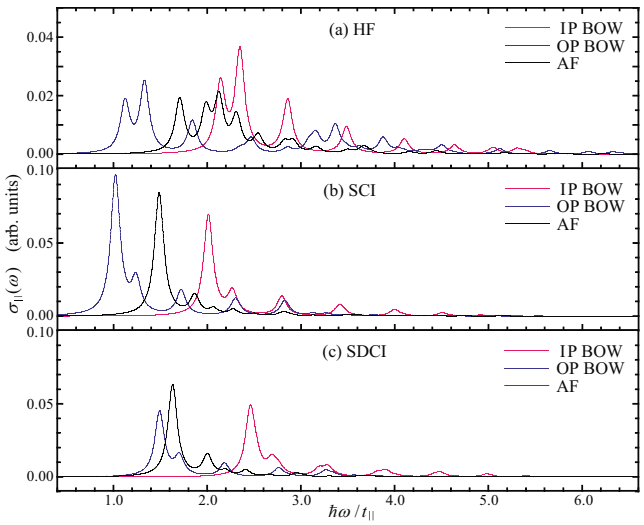

FIG. 2. (Color online) HF, SCI, and SDCI calculations of the long-axis-polarized optical conductivity spectrum for IP BOW, OP BOW, and AF at $N=16$ under the screened-Coulomb and moderate-coupling parameters. Every spectral line is Lorentzian broadened by a width of $0.06t_{\parallel}$.

IV. OPTICAL CONDUCTIVITY SPECTRA

We calculate the polarized optical conductivity spectra of energetically competing IP BOW, OP BOW, and AF with varying number of contributive Slater determinants and compare them in Fig. 2. First of all we are impressed with an optical contrast between IP and OP BOWs, which is noticeable even in the HF scheme. They are degenerate with each other in their energetics but distinguishable from each other in their optics. Their most intense peaks appear far apart and in between that of AF. The HF description of the relative intensity and position of each peak is much poorer than the CI findings, but it is useful enough to illuminate the optical nature of individual phases in a qualitative manner.

Based on the HF energy scheme, Fig. 3 analyzes the polarized optical conductivity spectra parallel and perpendicular to the conjugation direction. There are four molecular orbitals in each unit cell, and they are molded into two valence and two conduction bands fulfilling the electron-hole symmetry. The dispersion relations of IP and OP BOWs are exactly the same within the HF scheme and remain alike even with many-body Coulomb correlations fully considered.[18] Their dipole transition matrices are also the same, provided that the excitation light is polarized in the rung direction, as shown in Fig. 3(c), where most of the spectral weight comes from 2-to-3 interband transitions. It is due to the parity-definite molecular orbitals[14,43] that both 1-to-3 and 2-to-4 interband excitations make no contribution to the rung-direction optical conductivity. Under the reflection about the plane bisecting every rung bond, the valence and conduction bands labeled 1 and 3 are of symmetric char-

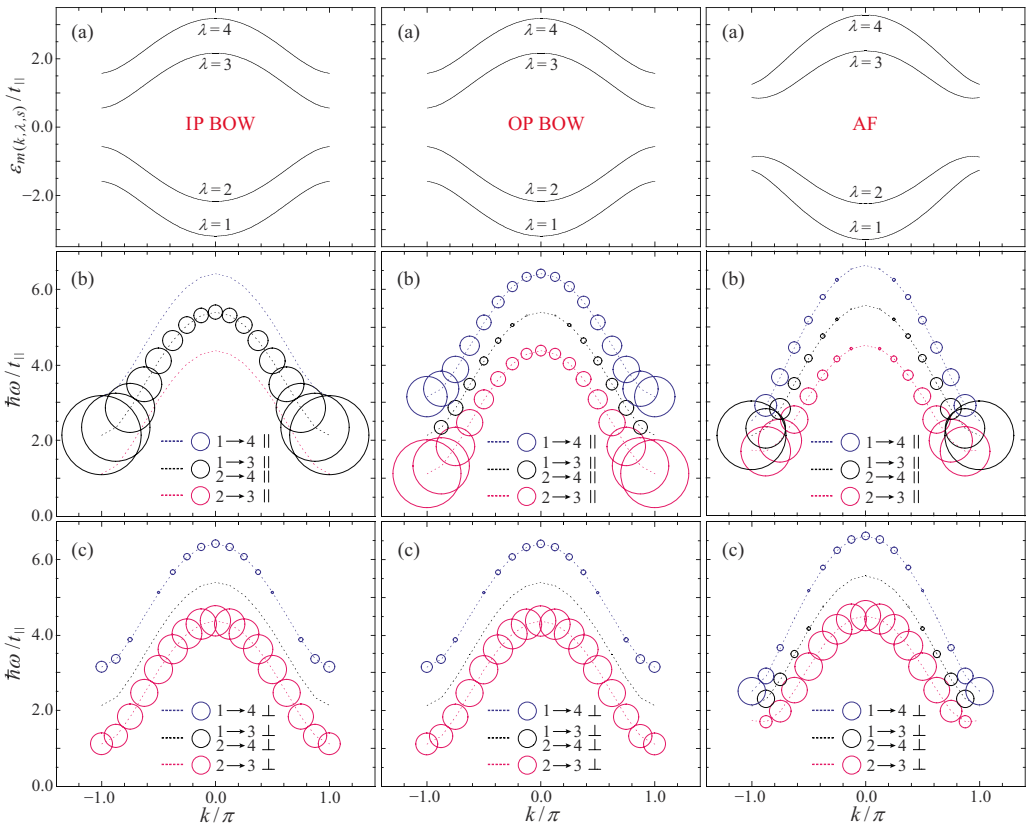

FIG. 3. (Color online) HF calculations of the dispersion relations of (a) the π-electron valence ($\lambda=1,2$) and conduction ($\lambda=3,4$) bands, and the "momentum-resolved" polarized optical conductivity (b) parallel and (c) perpendicular to the long axis for IP BOW, OP BOW, and AF at $N=16$ under the screened-Coulomb and moderate-coupling parameters, where the area of each circle corresponds to the spectral weight.

acter, whereas those labeled 2 and 4 are of antisymmetric character in both IP and OP BOWs. Any transition with parity unchanged is optically forbidden. On the other hand, photoirradiation in the conjugation direction reveals a striking contrast between IP and OP BOWs, as shown in Fig. 3(b), where all the spectral weight comes from 1-to-3 and 2-to-4 interband transitions in IP BOW, while there is little contribution from them in OP BOW. The conjugation-direction optical conductivity on an OP-BOW background arises mostly from 2-to-3 and 1-to-4 excitations.

The $\sigma_{\parallel}(\omega)$ spectra of IP and OP BOWs are thus distinguishable. Their main peaks sandwich the AF low-energy absorption bands (Fig. 2). With Coulomb correlations fully taken into account, the most intense absorption band is sharpened and grown up in general. Those of OP BOW and AF are close to each other, staying away from that of IP BOW. The screened-Coulomb and moderate-coupling parameters in our use stabilize AF slightly more than IP BOW. Band gaps are barometers of stabilization, and therefore AF is gapped wider than IP BOW [Fig. 3(a)]. Although the BOW Peierls gap is smaller than the AF Mott-Hubbard gap, the main absorption peak in the AF spectrum appears much below that in the IP-BOW one. This trick is due to the optically forbidden lowest-lying Peierls-gap excitation through a long-axis-polarized photon on an IP-BOW background.

The optical contrast between IP and OP BOWs is more and more accentuated with increasing coupling strength. If we reduce the elastic constant K to half the present value, as indicated with ○ in Fig. 1, the electron-lattice coupling is effectively strengthened and any distorted structure is sufficiently stabilized against the Mott insulator. It may be the case, for instance, with organic molecular compounds of alternating tetrathiafulvalene and chloranil[44] and/or halogen-bridged transition-metal linear-chain complexes.[45,46] Figure 4 shows the same calculations as in Fig. 3 but with $K=7.75$ eV/Å^2. In the case of electron-lattice interactions predominating over electron-electron correlations, both valence and conduction bands are much less dispersive in general and the long-axis-polarized dipole transitions between them are really eloquent of their background lattice distortion. In the conjugation direction, 1-to-4 and 2-to-3 dipole matrix elements vanish on an IP-BOW background, while those of 1 to 3 and 2 to 4 are negligibly small on an OP-BOW background. For light polarized in the rung direction, IP and OP BOWs similarly behave and their optical features are essentially given by 2-to-3 interband transitions.

We present in Fig. 5 the resultant polarized optical conductivity spectra. For light polarized in the conjugation direction, IP and OP BOWs exhibit a single and two well-separated absorption bands, respectively. With configuration interactions fully taken into account, the single IP-BOW absorption band consists of an intense peak and its satellite in the high-energy side, whereas a couple of the OP-BOW absorption bands are both single peaked, in a practical sense, due to the predominant zone-center excitations. Many-body electron correlations further have a significant effect on the relative intensity of the absorption bands. The spectral weight of the higher-energy OP-BOW absorption band turns out to be much smaller than that of the lower-energy one. For light polarized in the rung direction, IP and OP BOWs are

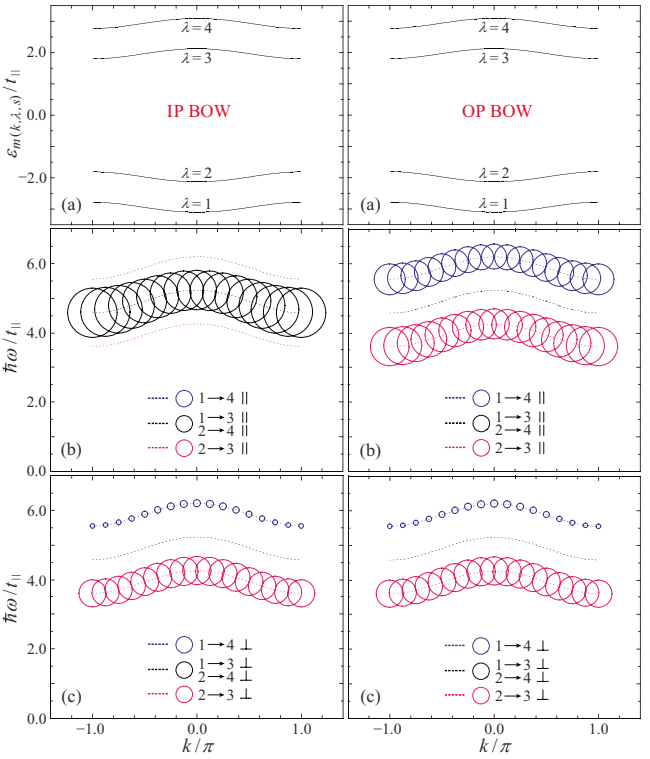

FIG. 4. (Color online) The same as in Fig. 3 but under the screened-Coulomb and strong-coupling parameters.

degenerate with each other. Their spectra slightly differ beyond the HF scheme, but the difference is hardly recognizable in practice. The common $\sigma_{\perp}(\omega)$ spectrum is peaked similarly as the IP-BOW $\sigma_{\parallel}(\omega)$ spectrum is, but high-energy absorptions are strongly suppressed in the rung direction.

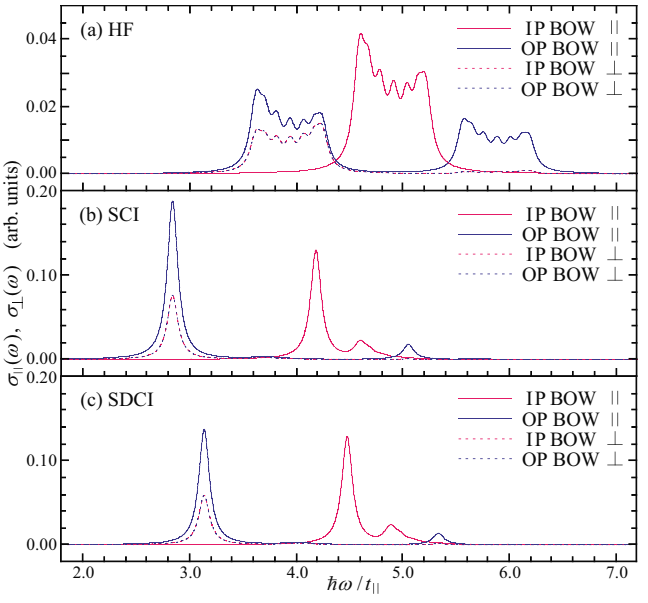

FIG. 5. (Color online) HF, SCI, and SDCI calculations of the polarized optical conductivity spectra parallel (∥) and perpendicular (⊥) to the long axis for IP and OP BOWs at $N=16$ under the screened-Coulomb and strong-coupling parameters. Every spectral line is Lorentzian broadened by a width of $0.06t_{\parallel}$.

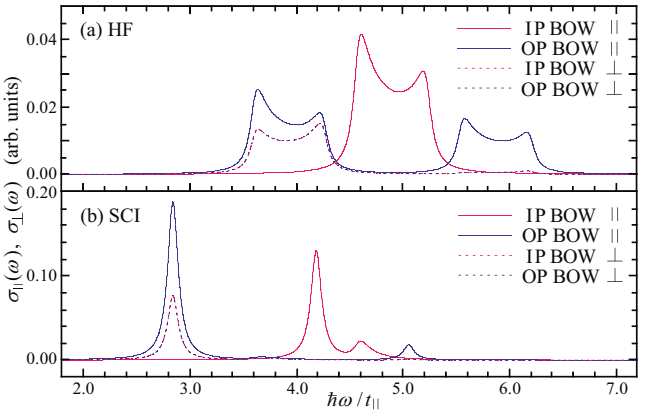

FIG. 6. (Color online) The same as in Fig. 5 but with $N=128$, where the SDCI scheme is never feasible.

Finally we stress that the present findings are not individual features of small oligoacenes but symbolize polyacene in the thermodynamic limit. All the features but irregular outlines peculiar to small clusters in Fig. 5 remain unchanged with further increasing conjugation length, as demonstrated in Fig. 6. Indeed the absolute location and the relative intensity of every absorption depend on the number of benzene rings,[23] but they are almost converging at $N=16$.

V. SUMMARY

We have optically characterized competing ground states of polyacene and revealed a striking contrast between the two highly degenerate Peierls-distorted states in particular. The *cis*- and *trans*-distorted structures, which we refer to as IP and OP BOWs, are almost degenerate in their energetics but quite distinct in their optics. The highest-occupied-molecular-orbital to lowest-unoccupied-molecular-orbital transition through a long-axis-polarized photon is allowed in OP BOW but forbidden in IP BOW. There appear two well-separated absorption bands against a background of OP BOW, and in between a single absorption band with an IP-BOW background sits. Such distinct features may not be demonstrated as they are in polyacene of predominantly strong electron-electron correlation, but with growing electron-lattice coupling they become detectable literally. We may consider heteroacenes such as paracyanogen,[47] as well as substituting hydrogen atoms in polyacene with larger molecules, in an attempt to tune the elastic properties and to realize a coupling-dominant situation.

The realistic set of parameters is located in close vicinity to a phase boundary, where an antiferromagnetic Mott-insulating state, which we refer to as AF, is slightly lower in energy and gapped wider than the two Peierls-distorted states. The most intense AF absorption peak nevertheless appears far below the IP-BOW absorption band for light polarized in the conjugation direction. For light polarized in the rung direction, on the other hand, the common optical gap of IP and OP BOWs is naively smaller than that of AF. The relative location of their main absorption peaks remains qualitatively unchanged with varying configuration interactions, though the excitonic effects on the optical spectra are significant in general.

There is another example[34] of optically characterizing distinct ground states in competition. Some class of platinum-halide ladder compounds exhibits Peierls-distorted CDW ground states of the IP and OP types. According to their interchain valence arrangements, their optical conductivity spectra are differently peaked. In this case, however, IP CDW and OP CDW not only look different in their energetics but also possibly present some contrast for the Raman spectroscopy. In the present case, IP and OP BOWs are so degenerate with each other that much effort has been devoted to solving the problem of which is energetically preferable.[15] Then the optical contrast between them will indeed come in useful in identifying them. Regular substitution of carbon atoms in polyacene, for instance, with nitrogen atoms, may lead to further stabilization of the Peierls-distorted structures against the aromatic one. IP and OP BOWs remain closely competing with each other in polypyridinopyridine.[47] We hope our calculations will stimulate a renewed interest in polycyclic aromatic hydrocarbons.

ACKNOWLEDGMENTS

The author is grateful to J. Ohara for fruitful discussion. This work was supported by the Ministry of Education, Culture, Sports, Science, and Technology of Japan.

[1] J. H. Schön, Ch. Kloc, A. Dodabalapur, and B. Batlogg, Science **289**, 599 (2000).
[2] M. A. Baldo, R. J. Holmes, and S. R. Forrest, Phys. Rev. B **66**, 035321 (2002).
[3] D. J. Gundlach, Y. Y. Lin, T. N. Jackson, S. F. Nelson, and D. G. Schlom, IEEE Electron Device Lett. **18**, 87 (1997).
[4] J. H. Schön, S. Berg, Ch. Kloc, and B. Batlogg, Science **287**, 1022 (2000).
[5] V. Y. Butko, X. Chi, D. V. Lang, and A. P. Ramirez, Appl. Phys. Lett. **83**, 4773 (2003).
[6] K. S. Novoselov, A. K. Geim, S. V. Morozov, D. Jiang, Y. Zhang, S. V. Dubonos, I. V. Grigorieva, and A. A. Firsov, Science **306**, 666 (2004).
[7] K. S. Novoselov, A. K. Geim, S. V. Morozov, D. Jiang, M. I. Katsnelson, I. V. Grigorieva, S. V. Dubonos, and A. A. Firsov, Nature (London) **438**, 197 (2005).
[8] Y. Zhang, Y.-W. Tan, H. L. Stormer, and P. Kim, Nature (London) **438**, 201 (2005).
[9] C. Berger, Z. Song, X. Li, X. Wu, N. Brown, C. Naud, D. Mayou, T. Li, J. Hass, A. N. Marchenkov, E. H. Conrad, P. N. First, and W. A. de Heer, Science **312**, 1191 (2006).
[10] N. M. R. Peres and F. Sols, J. Phys.: Condens. Matter **20**, 255207 (2008).
[11] L. Salem and H. C. Longuet-Higgins, Proc. R. Soc. London, Ser.

A **255**, 435 (1960).
[12] C. K. Chiang, C. R. Fincher, Jr., Y. W. Park, A. J. Heeger, H. Shirakawa, E. J. Louis, S. C. Gau, and A. G. MacDiarmid, Phys. Rev. Lett. **39**, 1098 (1977).
[13] H. C. Longuet-Higgins and L. Salem, Proc. R. Soc. London, Ser. A **251**, 172 (1959).
[14] M. Kertesz and R. Hoffmann, Solid State Commun. **47**, 97 (1983).
[15] M. Bendikov, F. Wudl, and D. F. Perepichka, Chem. Rev. (Washington, D.C.) **104**, 4891 (2004), and references therein.
[16] M. K. Sabra, Phys. Rev. B **53**, 1269 (1996).
[17] W. P. Su, J. R. Schrieffer, and A. J. Heeger, Phys. Rev. Lett. **42**, 1698 (1979); Phys. Rev. B **22**, 2099 (1980).
[18] C. Raghu, Y. Anusooya Pati, and S. Ramasesha, Phys. Rev. B **65**, 155204 (2002).
[19] B. Srinivasan and S. Ramasesha, Phys. Rev. B **57**, 8927 (1998).
[20] K. N. Houk, P. S. Lee, and M. Nendel, J. Org. Chem. **66**, 5517 (2001).
[21] M. Bendikov, H. M. Duong, K. Starkey, K. N. Houk, E. A. Carter, and F. Wudl, J. Am. Chem. Soc. **126**, 7416 (2004).
[22] J. Hachmann, J. J. Dorando, M. Avilés, and G. K.-L. Chan, J. Chem. Phys. **127**, 134309 (2007).
[23] P. Sony and A. Shukla, Phys. Rev. B **75**, 155208 (2007).
[24] Z. J. Li, H. Q. Lin, and K. L. Yao, Z. Phys. B: Condens. Matter **104**, 77 (1997).
[25] Z. J. Li, H. B. Xu, and K. L. Yao, Mod. Phys. Lett. B **11**, 477 (1997).
[26] Y. J. Wu, H. Zhao, Z. An, and C. Q. Wu, J. Phys.: Condens. Matter **14**, L341 (2002).
[27] Z. An and C. Q. Wu, Int. J. Mod. Phys. B **17**, 2023 (2003).
[28] Z. An and C. Q. Wu, Eur. Phys. J. B **42**, 467 (2004).
[29] H. Zhao, Z. An, and C. Q. Wu, Eur. Phys. J. B **43**, 53 (2005).
[30] K. Ohno, Theor. Chim. Acta **2**, 219 (1964).
[31] M. Chandross and S. Mazumdar, Phys. Rev. B **55**, 1497 (1997).
[32] K. B. Wiberg, J. Org. Chem. **62**, 5720 (1997).
[33] J. Ohara and S. Yamamoto, Phys. Rev. B **73**, 045122 (2006).
[34] S. Yamamoto and J. Ohara, Phys. Rev. B **76**, 235116 (2007).
[35] H. Ghosh, A. Shukla, and S. Mazumdar, Phys. Rev. B **62**, 12763 (2000).
[36] A. Shukla, Phys. Rev. B **65**, 125204 (2002).
[37] A. Shukla, H. Ghosh, and S. Mazumdar, Phys. Rev. B **67**, 245203 (2003).
[38] A. Shukla, Phys. Rev. B **69**, 165218 (2004).
[39] A. Shukla, Chem. Phys. **300**, 177 (2004).
[40] P. Sony and A. Shukla, Phys. Rev. B **71**, 165204 (2005).
[41] M. Kertesz, Y. S. Lee, and J. J. P. Stewart, Int. J. Quantum Chem. **35**, 305 (1989).
[42] J. Cioslowski, J. Chem. Phys. **98**, 473 (1993).
[43] S. Kivelson and O. L. Chapman, Phys. Rev. B **28**, 7236 (1983).
[44] K. Iwano, Phys. Rev. B **66**, 060302(R) (2002).
[45] M. Alouani, J. W. Wilkins, R. C. Albers, and J. M. Wills, Phys. Rev. Lett. **71**, 1415 (1993).
[46] K. Iwano, Phys. Rev. B **70**, 241102(R) (2004).
[47] M.-H. Whangbo, R. Hoffmann, and R. B. Woodward, Proc. R. Soc. London, Ser. A **366**, 23 (1979).